

REPORT DOCUMENTATION PAGE

Public reporting burden for this collection of information is estimated to average 1 hour per response, including gathering and maintaining the data needed, and completing and reviewing the collection of information, collection of information, including suggestions for reducing this burden, to Washington Headquarters Service, Paperwork Reduction Project (1218-0187), Washington, DC 20503.

1. AGENCY USE ONLY (Leave blank)		2. REPORT DATE 3/2/98	3. REPORT TYPE AND DATES COVERED FINAL TECH RPT, 01 Jan 95-31Dec97
4. TITLE AND SUBTITLE The Physical Origin of In-Cloud Lightning Processes Determined from Multiple-Station Wideband Electric Field Research.			5. FUNDING NUMBERS F49620-95-1-0114
6. AUTHOR(S) Dr. Ewen M. Thomson			
7. PERFORMING ORGANIZATION NAME(S) AND ADDRESS(ES) University of Florida 219 Grinter Hall P.O. Box 115500 Gainesville, FL 32611			8. PERFORMING ORGANIZATION REPORT NUMBER
9. SPONSORING/MONITORING AGENCY NAME(S) AND ADDRESS(ES) AFOSRINM 110 Duncan Ave., Suite B 115 Bolling AFB, DC 20332-0001			10. SPONSORING/MONITORING AGENCY REPORT NUMBER
11. SUPPLEMENTARY NOTES			
12a. DISTRIBUTION / AVAILABILITY STATEMENT Approved for public release; distribution unlimited.			12b. DISTRIBUTION CODE
13. ABSTRACT (Maximum 200 words) The overall objective was to understand better the physics of in-cloud lightning processes that give rise to radiation pulses in the electric field record. The most significant progress made was in the areas of theoretical development and analysis of 1992 data. The fundamental expressions for electric and magnetic fields from an extending lightning channel were shown to be incomplete. Specifically, a different interpretation of the classical electrostatic, induction and radiation components was found and a simpler expression for the far-field expression was derived. Electric field reversals were used to infer simultaneous development of multiple in-cloud channels. Electric field waveshapes were consistent with point sources for the first 200ns but not necessarily for longer times. Velocities of propagation are shown to vary with repeating processes in an intracloud flash. Two return strokes separated by less than a millisecond but both showing fine structure are located in spatially-separate channels at ground that joined a common channel higher up. A dart-stepped leader retraced the common channel section but became a stepped leader after emerging below cloud base.			
14. SUBJECT TERMS Electric Fields; Lightning: In-Clouds			15. NUMBER OF PAGES 21
			16. PRICE CODE 0
17. SECURITY CLASSIFICATION OF REPORT unclassified	18. SECURITY CLASSIFICATION OF THIS PAGE unclassified	19. SECURITY CLASSIFICATION OF ABSTRACT unclassified	20. LIMITATION OF ABSTRACT UL

NSN 7540-01-280-5500

Standard Form 298 (Rev. 2-89)
Prescribed by ANSI Std. Z39-18
298-102

19980326 029

DTC QUALITY INSPECTED 4

Final Technical Report

1. Cover Sheet

Date 2/20/98

**Title The Physical Origin of In-Cloud Lightning Processes
Determined from
Multiple-Station Wideband Electric Field Measurements**

**PI Ewen M. Thomson
Department of Electrical and Computer Engineering
PO Box 116200
University of Florida
Gainesville, FL 32611-6200**

Grant Number F49620-95-1-0114

Abstract

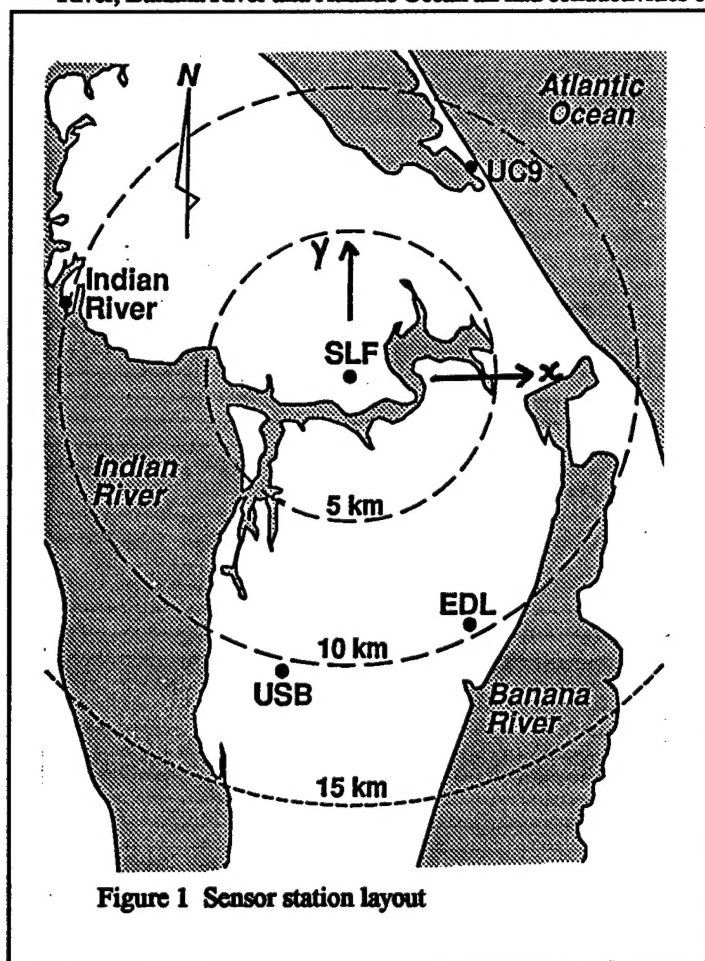
The overall objective was to understand better the physics of in-cloud lightning processes that give rise to radiation pulses in the electric field record. The most significant progress made was in the areas of theoretical development and analysis of 1992 data. The fundamental expressions for electric and magnetic fields from an extending lightning channel were shown to be incomplete. Specifically, a different interpretation of the classical electrostatic, induction and radiation components was found and a simpler expression for the far-field expression was derived. Electric field reversals were used to infer simultaneous development of multiple in-cloud channels. Electric field waveshapes were consistent with point sources for the first 200ns but not necessarily for longer times. Velocities of propagation are shown to vary with repeating processes in an intracloud flash. Two return strokes separated by less than a millisecond but both showing fine structure are located in spatially-separate channels at ground that joined a common channel higher up. A dart-stepped leader retraced the common channel section but became a stepped leader after emerging below cloud base.

Experiment

The original measurement system, established in 1991 and 1992, comprised five sensing stations in a network approximately 15 km x 15 km in size at Kennedy Space Center, Florida. The stations were located at the Shuttle Landing Facility (SLF), the eastern bank of the Indian river, the Universal Camera Site on Playalinda Beach (UC9), the Engineering Development Laboratory (EDL), and the Unified S-Band site (USB), as shown in the map of Fig. 1. In the following analysis, we refer to these as stations 1 through 5 respectively. The Indian River, Banana River and Atlantic Ocean all had conductivities of about 4 S/m. The Indian River and UC9

sensors were sited on well-conducting salt marsh (conductivity of about 2 S/m) while SLF, EDL, and USB were sited on stratified sand dunes with conductivities that we determine to be of the order of 10^{-2} S/m. During 1995 and 1996 we rebuilt all signal electronics but placed them at these same field sites.

The time derivative of the electric field, dE/dt was detected at each station by sensing the displacement current intercepted by a flat plate antenna. Gains from unity to 450 were achieved with different combinations of plates and amplifiers. Calibration signals were applied through a known resistance directly to the inputs of the dE/dt amplifiers to simulate a known dE/dt . The calibration signals included a square wave for absolute sensitivity determination, a triangle wave for linearity and saturation levels, an impulse (< 20 ns half width) and fast (< 30 ns 10-90% risetime) square wave for frequency response, and a horizontal synch pulse from Channel 35 TV in Orlando for timing. All gain and calibration controls were remotely controllable from the central recording station via two-way audio signals. Each dE/dt sensor plate was placed near the



center of a 3.5 m x 3.5 m conducting ground plane raised .5 m above local ground. The plates were connected to the sensor electronics, placed in a shielded box at one corner of the ground plane, via shielded 50 Ω coaxial cables routed below the ground plane. All signals passing to and from this box were electrically isolated from subsequent signal and communication links with fiber optics and optoisolators. Signals were sent back to the central recording station, that was 100 m away from the SLF ground plane, via either microwave links with a carrier of 10 GHz and 3 dB bandwidth of 1 MHz to 8 MHz, or analog fiber optics links with a 3 dB bandwidth of 1 MHz to 14 MHz. The signals were recorded at the central station in digital form using a 5-channel 8-bit Le Croy digitizing system interfaced with an 80386-based IBM clone PC. The signals were digitized at a rate of 20 MS/s for duration of 200 μ s each time a trigger event occurred at the central station. A trigger time, derived from Kennedy Space Center IRIGB with 1- μ s resolution, corresponded to the start of the 200- μ s recording window for each trigger event. Consecutive trigger events were digitized sequentially with a 40- μ s dead time between windows until the 128 kS Le Croy memory was full. Twenty-five trigger events could be recorded per lightning. A dead time of 1.5 s resulted when the digitized data for a 25-event lightning was transferred from Le Croy memory to computer RAM; hence, the initial pulses from virtually all lightnings in a storm could be recorded. Channel 1, corresponding to the sensor site at SLF, had a 32 μ s pretrigger delay so that pretrigger data could be recorded and the inherent delays in the signal links for the other channels meant that the signal radiated by the event that triggered the system was recorded somewhere in the 200 μ s window. The digital design of the 32- μ s delay in Channel 1 necessitated an additional anti-alias filter that reduced the frequency response of this channel to a 6-dB cutoff frequency of about 2 MHz the other channels had a 6-dB cutoff frequency of about 4 MHz. The digitizing system was activated 24 hours per day, with data being stored initially on a 1GB Winchester disk and later archived on optical disks.

In 1996, the system was updated to a 12-channel Le Croy system with essentially the same specifications as above except for an improved bandwidth – up to 10MHz on all channels – and simultaneous recording of dE/dt and electronically-integrated E. The extra channels were used to record VHF detected with an LDAR 66MHz receiver. Although several storm days of data were recorded in the summer of 1996, these have not yet been analyzed owing to programming problems.

Data

Since our data analysis has focussed on case studies of individual processes in particular lightnings, we have isolated the best data to this end. In Appendix A we present flash numbers, days, and major features of some of the data we have used so far. These were all recorded in 1992 on days when we had five-station calibrated data.

Exact expressions for E and B for propagating channel

The expressions for the electric and magnetic fields from a current in a propagating lightning channel form the basis for many models (for example, Lin et al., 1980; Uman, 1985; Nucci et al., 1990; and Thottappillil et al., 1993). Typically, in the derivation of these expressions, the explicit dependence on the charge density, introduced through the $\nabla\phi$ term, is removed using the Lorentz condition (for example, Rubinstein and Uman, 1989) although this is also possible through the continuity equation (Le Vine and Meneghini, 1983). However, in all previous derivations in the lightning literature the field expressions for an extending channel is obtained by modifying the expression for a fixed channel rather than deriving it from fundamentals. For a fixed channel, three distinct terms result. The “electrostatic” field varies as $1/R^2$, where r is the distance from source to field point, and involves the integral of current; the “induction” term varies as $1/R^2$ and involves current; the “radiation” term varies as $1/R$ and involves the time derivative of current. Hence at close distances the electric field can be approximated well by the electrostatic term and charge parameters can be interpreted from multiple-station measurements with sufficiently low frequency response (for example, ; Krehbiel et al., 1979; Koshak and Krider, 1989) and at far distances the radiation term can be interpreted in terms of current parameters (for example, Le Vine and Willett (1992)). No modeling has been done at intermediate distances using the induction term. For a propagating channel, or a travelling current discontinuity, Uman and McLain (1970) (see also correction in Rubinstein and Uman (1990)) deduced that an additional term needed to be added to the radiation term

in the magnetic field to account for the singularity in $\partial/\partial t$ that arises if the current turns on with a non-zero value at the tip of the propagating channel. Rubinstein and Uman (1991) introduce the turn-on term for the electric field the same way, that is, as an add-on term to the radiation component. In these treatments, the assumption is made that the partition of the electric field expression into electrostatic, induction, and radiation components is the same for a propagating channel as for a fixed channel apart from the additional term in the radiation expression.

We have derived the exact expressions for electric and magnetic fields, from fundamentals, assuming that the current is confined to a linear channel that is extending in an arbitrary direction, and show that the Lorentz condition can be obtained from the appropriate delayed-time form of the continuity equation. We obtain a different analytical form for the electrostatic term than that quoted extensively in the literature but show that the two forms appear to be equivalent at least to within a constant of integration. However, in order to obtain a simpler expression that we show to be equivalent to the "radiation" electric field quoted in the literature, we need to include a term that is clearly induction, that is, it varies with distance as $1/R^2$. Since this additional non-radiation term becomes insignificant at far distances, the far-field expression in the literature is still found valid, although it is strictly not a "radiation" field.

The details of these derivations are being submitted for publication. The main results are as follows. The electrostatic term

$$\bar{E}_s(\bar{r}, t) = -\frac{1}{4\pi\epsilon_0} \int_{t'=-\infty}^t \left[\int_0^{L'} \frac{\hat{l} - 3\hat{l} \cdot \hat{R}\hat{R}}{R^3} i\left(r, t' - \frac{R}{c}\right) d\tau' \right] dt'$$

differs from that commonly quoted in the literature (for example, Thottappillil et al., 1997) in the order of integration. However, the time derivative of these two expressions can be shown to be identical.

The induction component is

$$\bar{E}_I(\bar{r}, t) = -\frac{1}{4\pi\epsilon_0} \int_{t'=-\infty}^t \left[\begin{aligned} & \frac{\hat{l} - 3\hat{l} \cdot \hat{R}_{L'}\hat{R}_{L'}}{cR_{L'}^2} i\left(L', t' - \frac{R_{L'}}{c}\right) \frac{\partial L'}{\partial t'} \\ & + \int_0^{L'} \frac{\hat{l} - 3\hat{l} \cdot \hat{R}\hat{R}}{cR^2} \frac{\partial}{\partial t'} i\left(r, t' - \frac{R}{c}\right) d\tau' \\ & + \frac{1 - 2\hat{l} \cdot \hat{R}_{L'}^2}{c^2 R_{L'}^2} \hat{R}_{L'} \left[\frac{\partial L'}{\partial t'} \right]^2 i\left(L', t' - \frac{R_{L'}}{c}\right) \end{aligned} \right] dt'$$

where L' is the appropriate length of the channel at time t' taking into account delayed time effects and differs considerably from that appearing in previous work. Nevertheless, the first two terms can be combined to yield the commonly accepted form of the "induction" field

$$\begin{aligned} \bar{E}_I'(\bar{r}, t) &= -\frac{1}{4\pi\epsilon_0} \int_{t'=-\infty}^t \left[\frac{\partial}{\partial t'} \int_0^{L'} \frac{\hat{l} - 3\hat{l} \cdot \hat{R}\hat{R}}{cR^2} i\left(r, t' - \frac{R}{c}\right) d\tau' \right] dt' \\ &= -\frac{1}{4\pi\epsilon_0} \int_0^{L'} \frac{\hat{l} - 3\hat{l} \cdot \hat{R}\hat{R}}{cR^2} i\left(r, t - \frac{R}{c}\right) d\tau' \end{aligned}$$

Note that $\bar{E}_I'(\bar{r}, t)$ omits the third term in the equation for $\bar{E}_I(\bar{r}, t)$ that is a true induction term since it varies as $1/R^2$.

The radiation component, \bar{E}_R , comprises remaining five terms that can be combined into a single expression only if the induction component that we left out of the expression for $\bar{E}_I(\bar{r}, t)$ is added. Then we get a single-term expression

$$\bar{E}_R'(\bar{r}, t) = -\frac{1}{4\pi\epsilon_0} \frac{\partial}{\partial t} \left(\int_0^L \frac{\hat{l} - \hat{l} \cdot \hat{R} \hat{R}}{c^2 R} i \left(r, t - \frac{R}{c} \right) dL \right)$$

This simple expression is a good approximation for the electric field when $R \rightarrow \infty$, or, more quantitatively, when the longest time scale of interest is much shorter than R/c . For example, in the multiple-station dE/dt measurements made by Thomson et al., 1994 where pulse waveshapes have little variation after several microseconds, sources much more distant than about a kilometer have negligible electrostatic or induction components. Note however that the pure radiation field is a much more complicated expression containing five terms. If we expand the far-field expression $\bar{E}_R'(\bar{r}, t)$ into two terms

$$\bar{E}_R'(\bar{r}, t) = -\frac{1}{4\pi\epsilon_0} \left\{ \frac{\partial L}{\partial t} \frac{\hat{l} - \hat{l} \cdot \hat{R}_L \hat{R}_L}{c^2 R_L} i \left(L, t - \frac{R_L}{c} \right) + \int_0^L \frac{\hat{l} - \hat{l} \cdot \hat{R} \hat{R}}{c^2 R} \frac{\partial}{\partial t} i \left(r, t - \frac{R}{c} \right) dL \right\}$$

then the first term corresponds to the "turn-on" term introduced by Uman and McLain (1970) and corrected by Rubinstein and Uman (1990). A major motivation for this theoretical work was the need to interpret the multiple-station dE/dt measurements made by Thomson et al. (1994) in terms of sources that have arbitrary orientation. Since there are no explicit formulations for dE/dt in the literature, we attempted to use those existing expressions for E but found ambiguities that needed elucidation. For example, in Le Vine and Willett (1992), who ignore the turn-on term, the partial derivative in the second term in the above expression for $\bar{E}_R'(\bar{r}, t)$ is described as being "with respect to the argument of the function enclosed" the function being the delayed current I , whose argument appears to be

$$t - \frac{\hat{l} \cdot \hat{R}}{v} - \frac{R}{c} \text{ where } v \text{ is the speed of propagation of the current pulse along an existing channel. As is}$$

apparent from the above derivation, the correct derivative is that with respect to time. We reached a similar conclusion from the citation used by Le Vine and Willett (1992) – Le Vine and Meneghini (1983).

In the light of the far-field expression $\bar{E}_R'(\bar{r}, t)$, we can now obtain dE/dt for a distant source as

$$\frac{d\bar{E}_R'(\bar{r}, t)}{dt} = -\frac{1}{4\pi\epsilon_0} \frac{\partial^2}{\partial t^2} \left(\int_0^L \frac{\hat{l} - \hat{l} \cdot \hat{R} \hat{R}}{c^2 R} i \left(r, t - \frac{R}{c} \right) dL \right)$$

Reversal effects in dE/dt waveshapes

Our original objective was to find the source dI/dt and velocity by applying the transmission line model to our five dE/dt measurements obtained on day 254, 1992. However, following the PI's suggestion, Hager and Wang (1995) concluded that the velocity was not readily found by simply inverting the relevant equations in Le Vine and Willett (1992) when 2% measurement errors were present in simulated data. In an effort to find another way to interpret the source physics, our subsequent investigation of reversal effects (Davis and Thomson, 1995) showed that dE/dt pulse polarities were mainly consistent with current flow along the apparent channel connecting pulse sources, in contrast with the "radio diameter" concept proposed by Proctor (1981) wherein the sources of VHF radiation tend to align across the line of source-source propagation. However, in some instances we found that the path connecting adjacent (in time) pulses was not a possible channel for current flow. For example, Fig. 2 shows five-station dE/dt waveshapes for a pulse train in an intracloud flash in which the Station 4 pulses change from near zero amplitude to negative, and the Station 5 pulses are a mixture of positive polarity, negative polarity, and near zero amplitude. Fig. 3 shows the corresponding locations with numbers indicating their time order of occurrence. After testing whether the observed pulse polarities were consistent with current flow along each path joining two pulse sources, we concluded that the paths joined by the dashed lines were not possible and hence that the lightning channel was branched at location #2 (or perhaps location #1), with one branch along the path 2-3-5-6 and the other along the path 2-4-7. Note that both channel branches are active simultaneously with pulses 3-4-5 alternating between branches. Thomson (1995) also found

that sequential pulse sources alternated between channels in the initial 2ms of a ground flash with an extensive prestroke in-cloud discharge phase. Hence we have established a novel technique that can be used to identify whether pulse sources are on different channels.

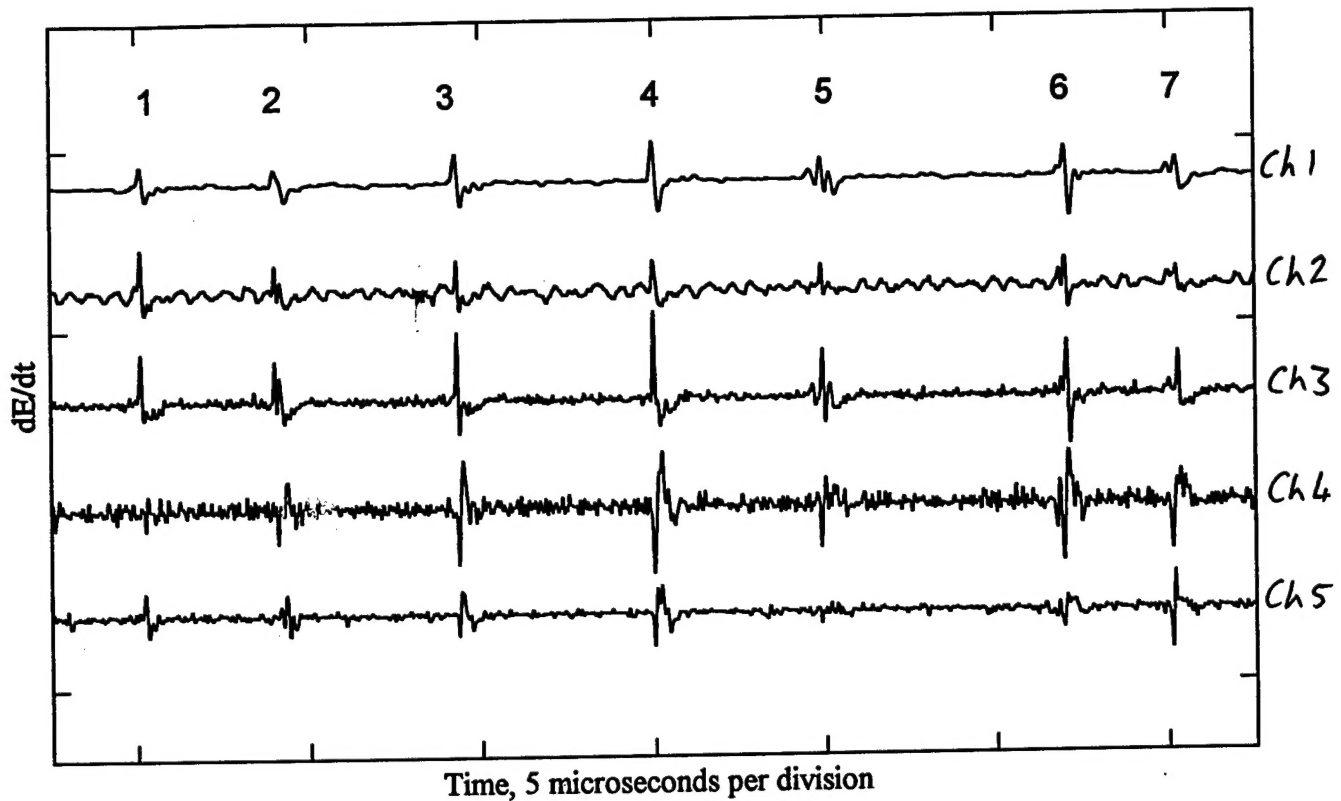


Figure 2 dE/dt waveshapes recorded at five stations

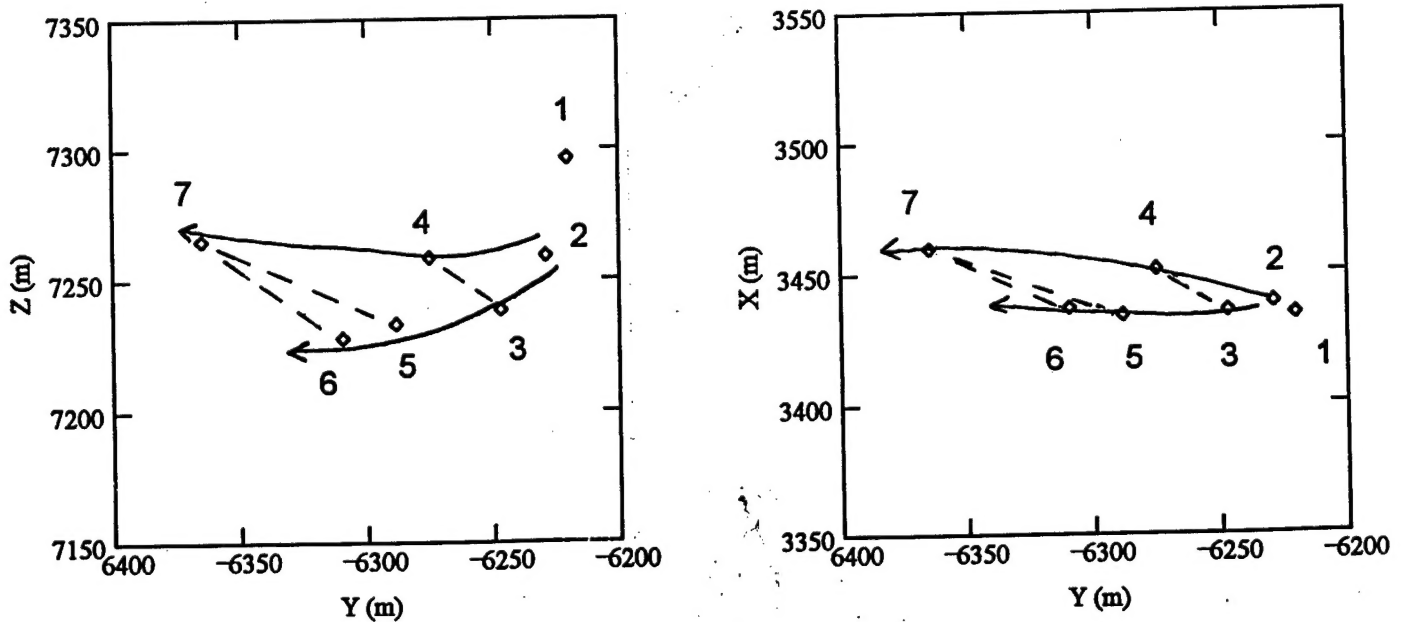


Figure 3 Locations for the seven pulses in Fig. 2

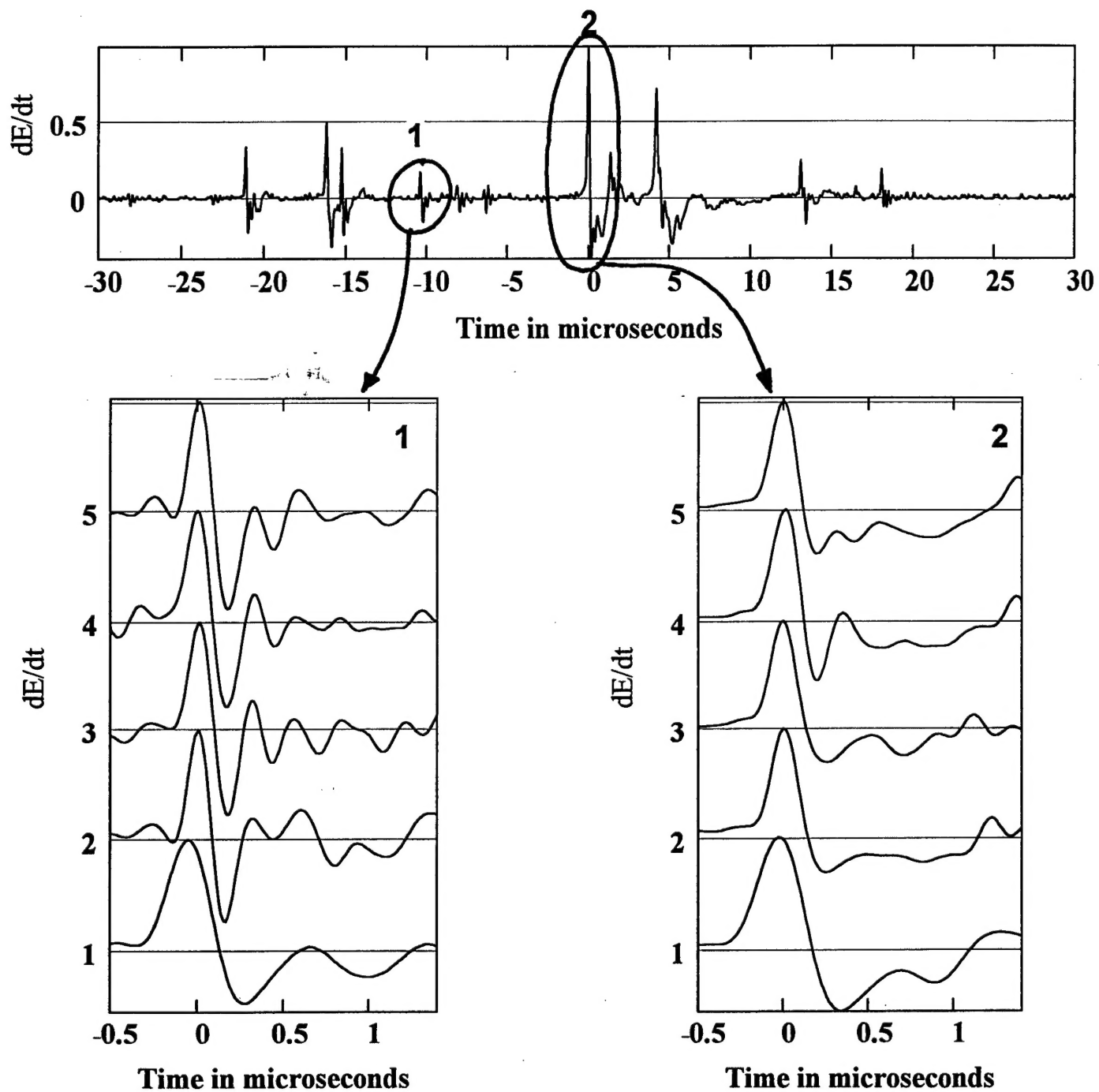


Figure 4 dE/dt pulses waveshapes in bipolar pulse in C-G flash #254/2979

Properties of electric field pulse waveshapes

The relationship between an electric field and its sources is well established (for example, Wangsness, 1986). If the current distribution is known, the electric field can be found. In practice the current is not known and the main problem is how to invert the measured fields to estimate the current. To this end, models have been developed that make various simplifying assumptions as to the form of the current distribution. Of the many current distribution models that have been applied to return strokes, Thottappillil and Uman (1993) found that one of the simplest, the transmission line model, predicted the peak fields the most reliably. In the transmission line model (for example, Uman and McLain, 1970; Le Vine and Meneghini, 1978; Willett et al., 1988; Rubinstein and Uman, 1990; Le Vine and Willett, 1992), a current pulse $I(t)$ propagates at constant velocity v along a channel without changing its waveshape. Hence the current at a distance l along the channel is of the form $I(t-l/v)$. The radiated electric field has sources only at the channel endpoints where the current turns on and off, and, for intervals shorter than the travel time along the channel, the electric field waveshape is identical to the current waveshape. Hence when E , or dE/dt , is measured at multiple stations, the waveshapes should all be the same. Fig. 4 illustrates some interesting points regarding dE/dt pulse waveshapes. The top plot shows all pulses in a pulse sequence whose integral, E (not shown), has the characteristic features noted by Weidman and Krider (1979) in bipolar pulses that occur early in both cloud and ground flashes - several small pulses followed by one (or two as here) large pulses and an overshoot. This sequence occurred in the second trigger event in a ground flash with extensive in-cloud activity preceding the first stroke. The two bottom plots are the dE/dt waveshapes for all five stations corresponding to the pulse annotated as "1" and "2" in the top plot. With the exception of the bottom dE/dt trace, which has smaller bandwidth than the others, all initial peaks in each pulse set have almost identical shapes. In the smaller pulse #1 this is also true of the overshoot, but the large amplitude pulse #2 has differently shaped overshoots for different stations. These similarities in waveshape around the peak indicate that dilation effects are probably insignificant for the initial 200 ns or so, consistent with the transmission line model. Further evidence of close agreement between stations in the waveshape near peak can be found in the low values of χ^2 found using the technique described in Thomson et al. (1994) wherein time-tags and timing errors are determined from initial peak features corresponding to rising-edge half width, peak, and falling-edge half width. Locations are found assuming a point source. Typically, timing errors are of the order of 20 ns and χ^2 are less than unity. Hence dilation effects are about or less than 10 ns and dE/dt sources appear to be point rather than spatially distributed. The same is apparently not always true, however, for the pulse overshoots.

Influence of channel conditioning on discharge physics

When considering the discharge physics of lightning processes, loosely termed as "streamers", that either form new channels, such as the stepped leader, or travel down previously formed channels, such as the dart stepped leader, two main aspects of streamer formation are of interest - the overall streamer-tip propagation, as determined from pulse-pulse source displacements, and the physics of individual pulse sources at the streamer tip. Both of these are influenced by channel conditioning as determined primarily by the interval since the last activity in the same channel as located using LDAR and wideband pulses. In ground flashes stepped leaders propagate at about $10^5 - 10^6$ m/s (Schonland, 1956), dart leaders at about 10^7 m/s (Orville and Idone, 1982), and return strokes at about 10^8 m/s (Schonland et al., 1935). Initial streamers in cloud flashes proceed at a similar speed to stepped leaders (Proctor, 1981; Taylor, 1978; Holmes et al., 1980; Mazur and Rust, 1983). Fig. 5 demonstrates some interesting features of streamers propagating in previously active in-cloud channels. The sources in this figure were found from three pulse trains (similar to those described in Krider et al., 1975) (numbered "1", "2" and "3" in order of occurrence) whose sources traversed common paths in a manner characteristic of K streamers, in the later stages of an intracloud flash. Gaps in the plots arise from dead time between trigger events and are not necessarily real. Note that the average speed determined from pulse-pulse displacements increases from traversal to traversal, with speed initially faster in the first and third but fairly uniform through the second. The third traversal is particularly interesting in that three linear regions are discernible in the distance versus time plot, with approximately steady speeds of 7.9×10^6 m/s, 3.6×10^6 m/s, and 1.6×10^6 m/s respectively, where the two transition points appear to be at the end of the channel defined by the first and second traversals. Another interesting point is that the intervals between

traversals are 43 ms and 35 ms, both much shorter than the 80 ms interval quoted by Proctor (1997) before channels are observed to reradiate at VHF. However, the channel conditioning in the first traversal did appear to influence the speed of the third traversal 78 ms later. Further, these pulse trains (or, more correctly, "source trains", since they are the sources of the pulse trains) propagated away from the flash origin, effectively transporting negative charge in this direction, in contrast to Shao and Krehbiel's (1996) observation that k streamers propagated, and transferred negative charge, towards cloud flash origins. All of these points merit further investigation.

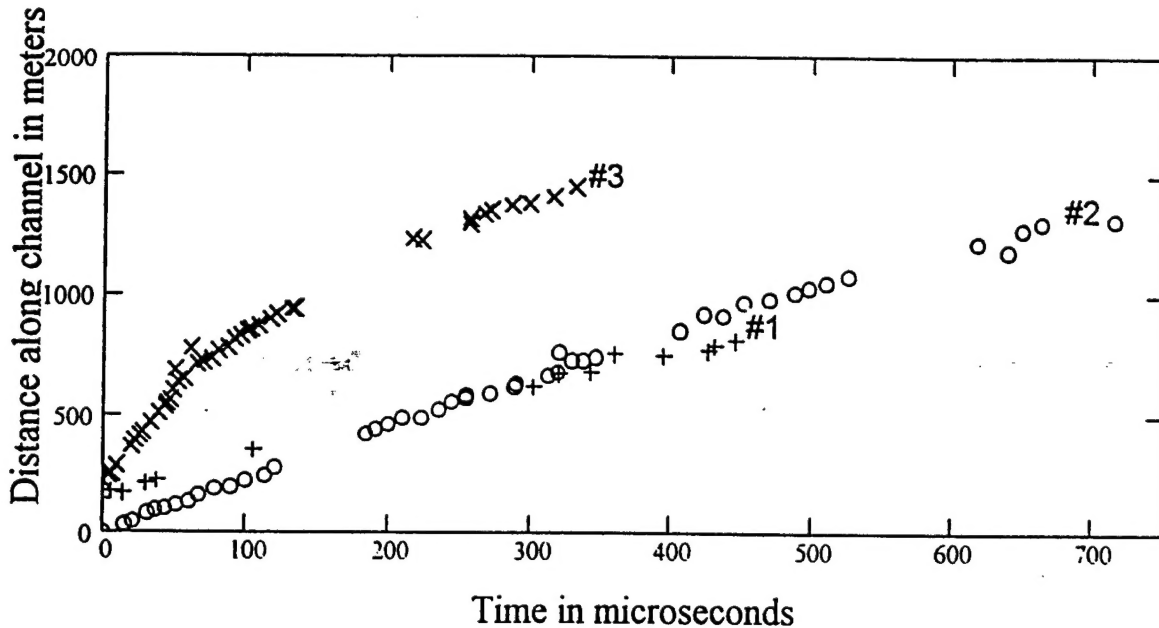


Figure 5 Distance along channel versus time for three consecutive source trains in intracloud flash

First return stroke waveforms separated by 1 ms or less

Weidman and Krider (1978) suggest that the large subsidiary peaks, or fine structure, present in the radiation fields from first strokes to ground are due to the effects of branches. When the return stroke current wavefront reaches the end of a branch formed by the previous stepped leader or changes velocity at a branch point, it may give rise to a change in the measured electric field, hence contributing to the structure after the initial return stroke peak. Willett et al. (1995) classify return strokes as being first or subsequent based on the return stroke radiation field waveform. One type of waveform was termed first stroke type and consisted of multiple jagged peaks in the E field and noisy in dE/dt . The other type of waveform was termed subsequent type and was smoothly rounded in E and quiet in dE/dt after the initial peak. All first stroke type waveforms were associated with first strokes or new terminations to ground while all subsequent stroke waveforms were radiated by old channels. Guo and Krider (1982) recorded two first stroke type waveforms separated by tens of microseconds. They suggest that these waveforms could have been produced by two ground terminations originating from the same stepped leader. Rakov and Uman (1994) recorded two first stroke type waveforms separated by hundreds of microseconds. Unlike Guo and Krider (1982), Rakov and Uman (1994) find evidence of only one channel to ground and conclude that the two waveforms were produced by two strokes down the same channel. This conclusion contradicts the hypothesis of Willett et al. (1995) concerning the origin of the fine structure since the first stroke would have neutralized the charge deposited by the first leader and any subsequent leader down the same channel would not be branched.

All of the studies mentioned employ video records to determine the number of channels produced by a discharge. Unfortunately this is not foolproof as a channel may be hidden from view of the camera if it occurs in a rain shaft or is displaced some distance away from another channel in the flash. Hence, the two first stroke type waveforms recorded by Rakov and Uman (1994) with a single visible channel may have been produced by two channels to ground with the second hidden from view.

In a case study of Flash 24200770 we recorded two first-stroke-type waveforms separated by 800 μ s and determined based upon their locations that their channels were spatially resolved. Furthermore we located the fine structure associated with each and find locations in the vicinity of each strike point, presumably due to the branches formed by the stepped leader. Flash 24200770 occurred at 17:36 hrs on day 242 during the summer of 1992. The flash was a multiple channel ground discharge located 15 km east and 4 km north of our central recording station at the Shuttle Landing Facility at Kennedy Space Center, FL. The locations of all sources obtained during this flash are shown in Fig. 7. The discharge produced 6 strokes to ground in 3 spatially separate terminations. The first sources detected in the flash were three sources due to the stepped leader near 6.3 km in height. At $t+200\mu$ s, $t+2$ ms, and $t+3$ ms, additional stepped leader sources were located and progressed earthward from 6.2 km, 5.8 km, and 5.7 km in altitude respectively, where "t" is the reference absolute time tag of the flash. Stepped leader sources are shown as circles in figure 1. The average downward velocity of the stepped leader from 6.3 km to 5.7 km in height was 2.2×10^5 m/s. At $t+48.2$ ms a first stroke type waveform was recorded and its location is shown as a circle marked "1". Six hundred microseconds later another first stroke type waveform was recorded and its location is shown as a circle marked "2". Several pulses in the fine structure associated with each stroke were located. Locations of these sources are shown in Fig. 6 and labeled according to their associated stroke.

Guo and Krider (1982) describe two first stroke field changes separated by tens of microseconds and suggest that they may be due to multiple contacts to ground by different branches of the same stepped leader. They further argue that the second branch must be within 5-40 m of ground when the first contacts ground otherwise the ensuing return stroke would travel up the trunk and out along the second branch and discharge it without producing a second termination to ground. The study by Rakov and Uman (1994) describe two first stroke type waveforms separated by hundreds of microseconds. Video records show only one channel to ground during this time. The mechanism described by Guo and Krider (1985) is insufficient to account for two strokes separated by hundreds of microseconds. Rakov and Uman (1994) conclude that the two first stroke waveforms were produced by consecutive strokes down the same channel. This argument contradicts the observations of Willett et al. (1995), namely that first stroke type waveforms are always produced by new terminations to ground. We find in flash 24200770 two first stroke type waveforms separated by 800 μ s and are located 1.2 km apart on the ground. Fig. 7 shows the waveforms for both of these strokes. Of interest here is the difference in duration of the fine structure - longer than 140 μ s for the first strike (top plot) and 65 μ s for the second. Locations of sources during the fine structure are above the respective strike points as shown in Fig. 6 and are marked on the time domain waveform in Fig. 7. The fine structure appears to be due to effects of branches of the stepped leader preceding each stroke and is located near earlier sources of the stepped leader, consistent with Weidman and Krider's and Willett's hypothesis but in apparent contradiction to the observations of Rakov and Uman (1994). The location of the highest fine structure source associated with the second stroke is marked on the time domain waveform of the second stroke in Fig. 7. Since this point is at a height of only 2.5 km, it is possible that at this point the return stroke from the second stroke has reached a point where there are no more branches. This would be the case if the second stroke were branched off the main channel which contained the first stroke. The fact that the fine structure of the first stroke is 2-3 times longer in duration than the second supports this view of a common stepped leader channel.

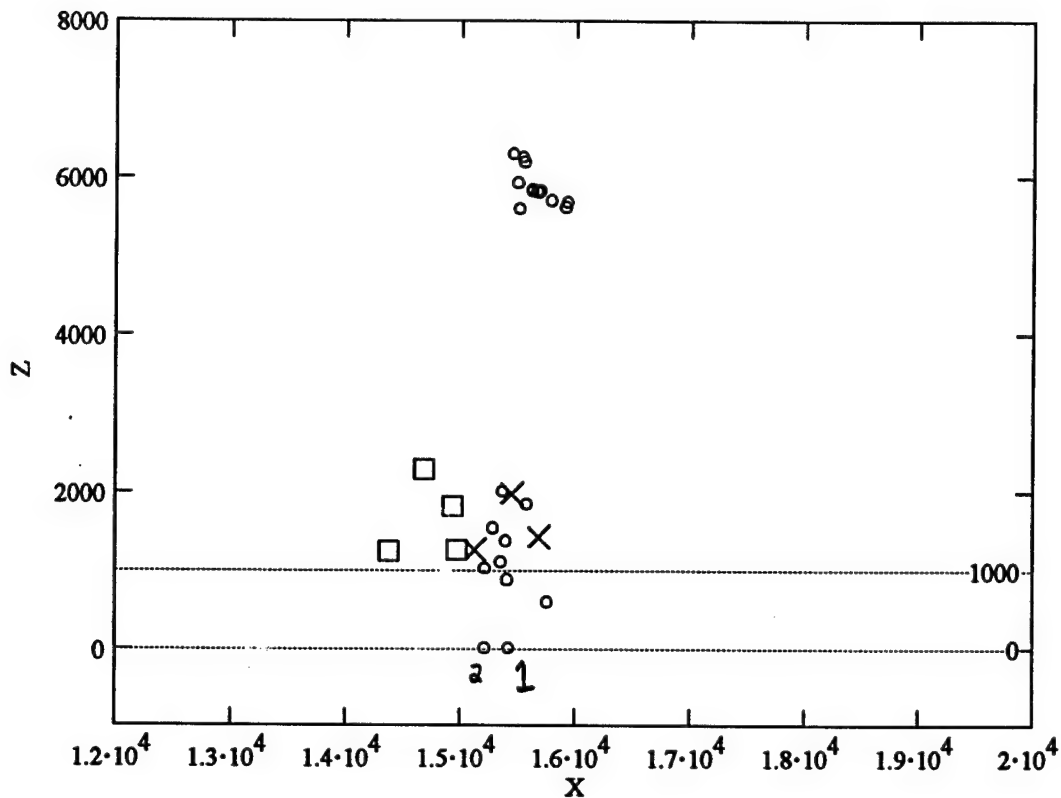
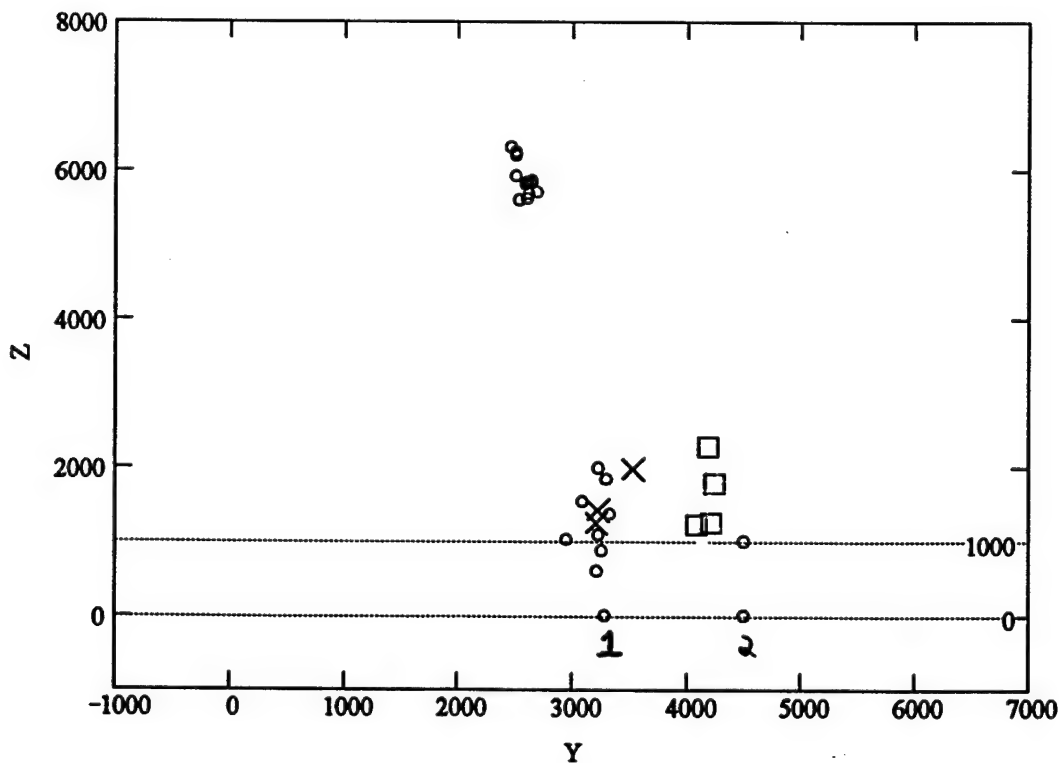


Figure 6 Locations of dE/dt sources for the first two strokes in flash 24200770. Stepped leader sources shown as circles. The two return strokes are labeled "1" and "2". Fine structure from the first stroke is denoted by "X"s. Second stroke fine structure shown as boxes.



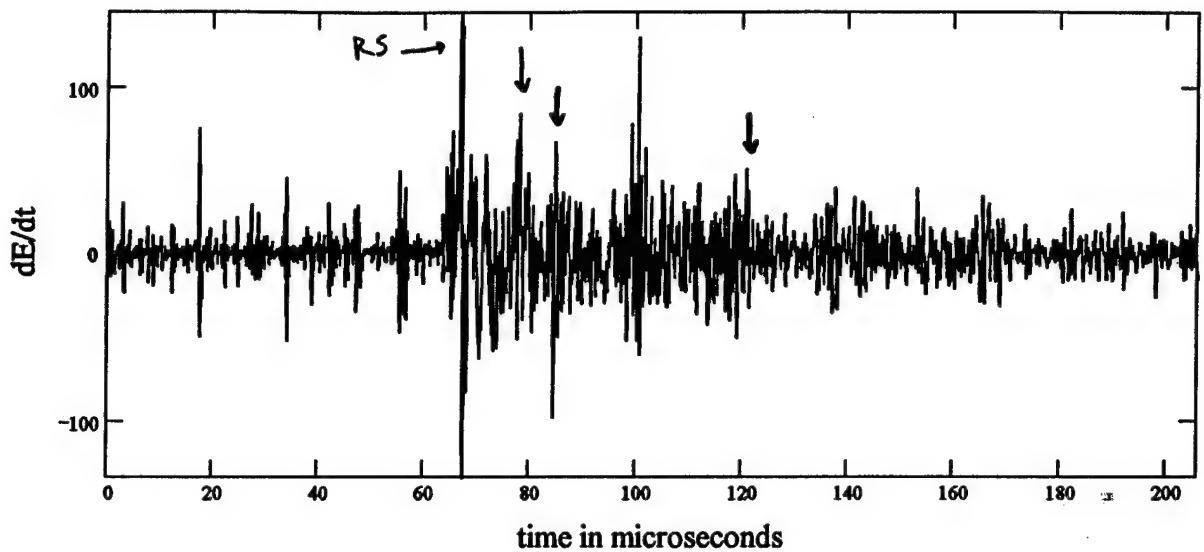
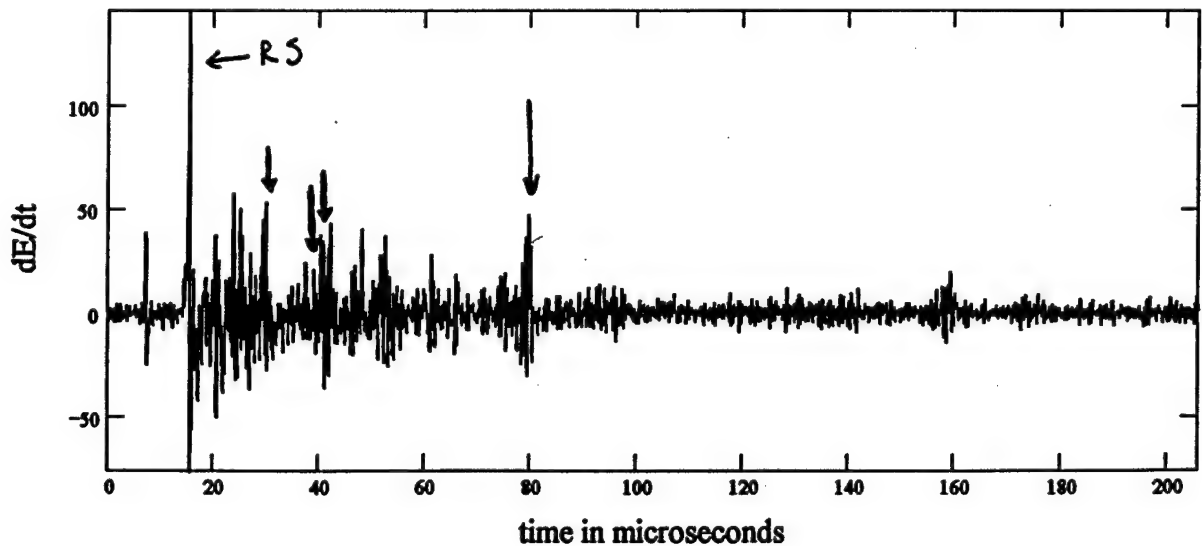


Figure 7 dE/dt waveforms for the first two strokes in figure 1. The strokes occurred 800 microseconds apart and were located 1.2 km apart. The main return stroke peaks are marked "RS" as well as locations obtained during the fine structure.



Leaders preceding new terminations to ground

Thomson et al. (1984) suggest that multiple channels below cloud base may be due to a subsequent leader following an old channel in cloud and then branching before reaching the cloud base and hence forming a new termination to ground. Rakov and Uman (1990c) report mean leader durations for new terminations to ground of 15 ms. This time is intermediate to that of subsequent leaders following the same channel as the preceding stroke, 1.8 ms, and that of leaders of first strokes, 35 ms. This observation is consistent with that of Thomson regarding a common origin in the cloud with the leader being faster when propagating over an old channel section and slowing down when forming a new channel. In flash 2420770 at $t+195$ ms (145 ms after the two first strokes), we recorded a pulse train which lasted for 3 ms and progressed earthward from 5.5 km to 0.8 km in height. Locations obtained for pulse train sources are shown in Fig. 8 where we have also included the initial stepped leader sources and the first two return stroke locations for reference. The average 3-dimensional point-to-point track velocity for the pulse train ranged from 2.9×10^6 m/s over the upper portion of the channel to 1.5×10^6 m/s over the final portion. These velocities are similar to those measured for dart-stepped leaders (Orville and Idone 1982, Schonland 1956) propagating in a previously ionized channel. Five milliseconds after the last source in the pulse train was located a first stroke type waveform was recorded and its location is marked as a diamond and labeled "3" in Fig. 8. We postulate that the leader continued to propagate to ground after the final sources we detected in the pulse train but did so as a stepped leader which we did not detect. (Stepped leader pulses are typically of smaller amplitude than dart-stepped leader pulses and hence less likely to trigger our system.) The waveforms for the last 430 μ s of the pulse train are shown in Fig. 9. Notice the decrease in amplitude after the 80 μ s mark in the lower trace. At this point the leader probably becomes stepped and the amplitude of the pulses decrease below our trigger threshold. We can estimate the velocity of this stepped leader from the location of the last source in the pulse train and the time to the return stroke. This average velocity is 2.3×10^5 m/s which is consistent with a stepped leader velocity and with that of the earliest sources we detected in the flash which were also stepped leader sources. The transition from dart-stepped leader to stepped leader in this case occurs near 1 km that is the height of the cloud base in Florida (Orville and Idone 1982). We have noted a similar behavior in other leaders, that is, a sudden transition from dart-stepped to stepped near the height of cloud base which suggests a fundamental change in the leader discharge mechanism as a result of the cloud/air boundary.

Fine structure of new termination to ground

Willett et al. (1995) report one case of an "anomalous" stroke which began as a first stroke (noisy dE/dt) and became quiet after 12 μ s. The hypothesis proposed by Willett et al. (1995) is that a new channel to ground off a previously illuminated channel would radiate a first stroke type waveform as it travels over the stepped leader forming this new channel and would then become quiet once it joined the existing channel formed by a previous stroke.

The waveform for the new termination to ground in flash 24200770 is shown in Fig. 10. The fine structure for this stroke is approximately 40 μ s in duration, shorter than for the first two strokes in the flash. Locations for the fine structure from this stroke is shown in Fig. 11 where we have included all of the dE/dt sources from the flash. Note from Fig. 11 that the fine structure locations (large diamonds) from the new termination do not coincide with the end of the preceding leader which we might expect to be the transition from a previous channel to a new stepped leader channel. One possible reason for the discrepancy is due to larger errors in the locations of the fine structure sources than for other sources in the flash. This is due to the complexity in the field structure and the difficulty in determining common sources on multiple traces. Another reason for the discrepancy is that the fine structure may be due to radiation from the tips of branches, as suggested by Weidman and Krider (1978) and may originate at locations off the main channel and hence not coincide with the joining of a new channel to an old one.

When viewing the sources from the first two strokes in the flash in the context of sources received later, we can begin to formulate a more complete picture of this discharge. The first stroke appears to be a branch off the main channel near 2 km high. Fine structure for this stroke lasted for at least 140 μ s. Locations of the fine structure are near that of the preceding stepped leader sources and lead to the branch off the main channel at 2 km. Unfortunately locations for later sources in the fine structure

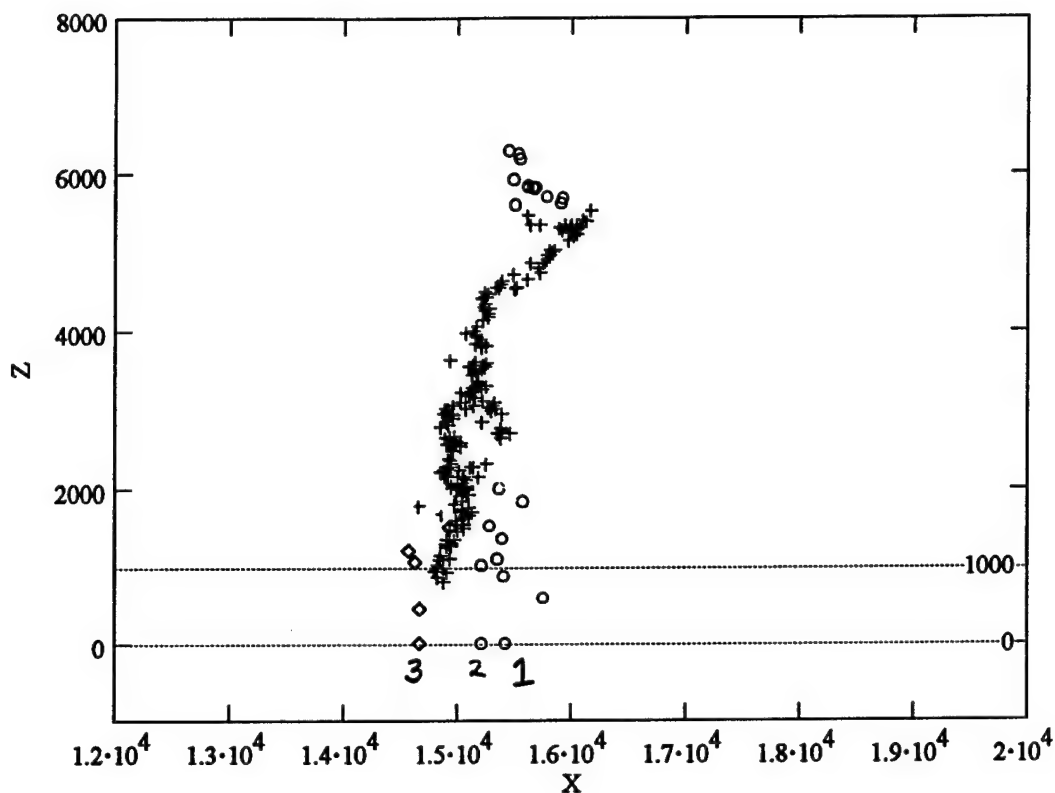
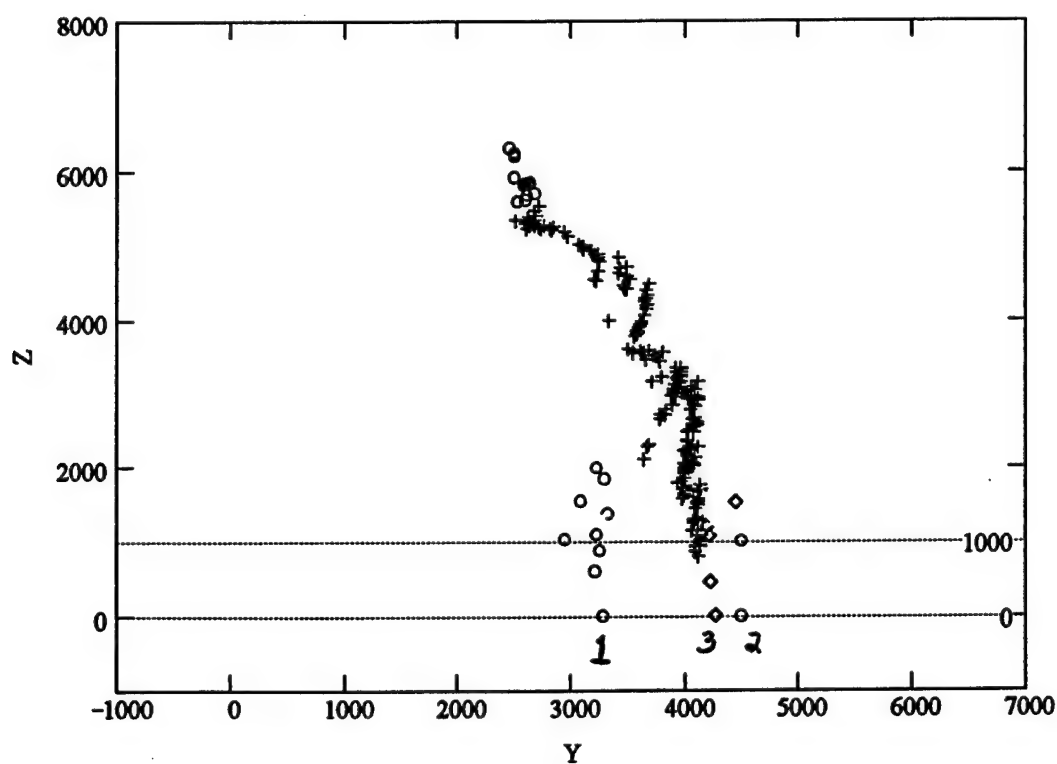


Figure 8 Locations of dE/dt sources preceding a new termination to ground in flash 24200770. Pulse train source locations shown as +s. Stepped leader sources immediately prior to new termination shown as diamonds. New termination is labeled "3".



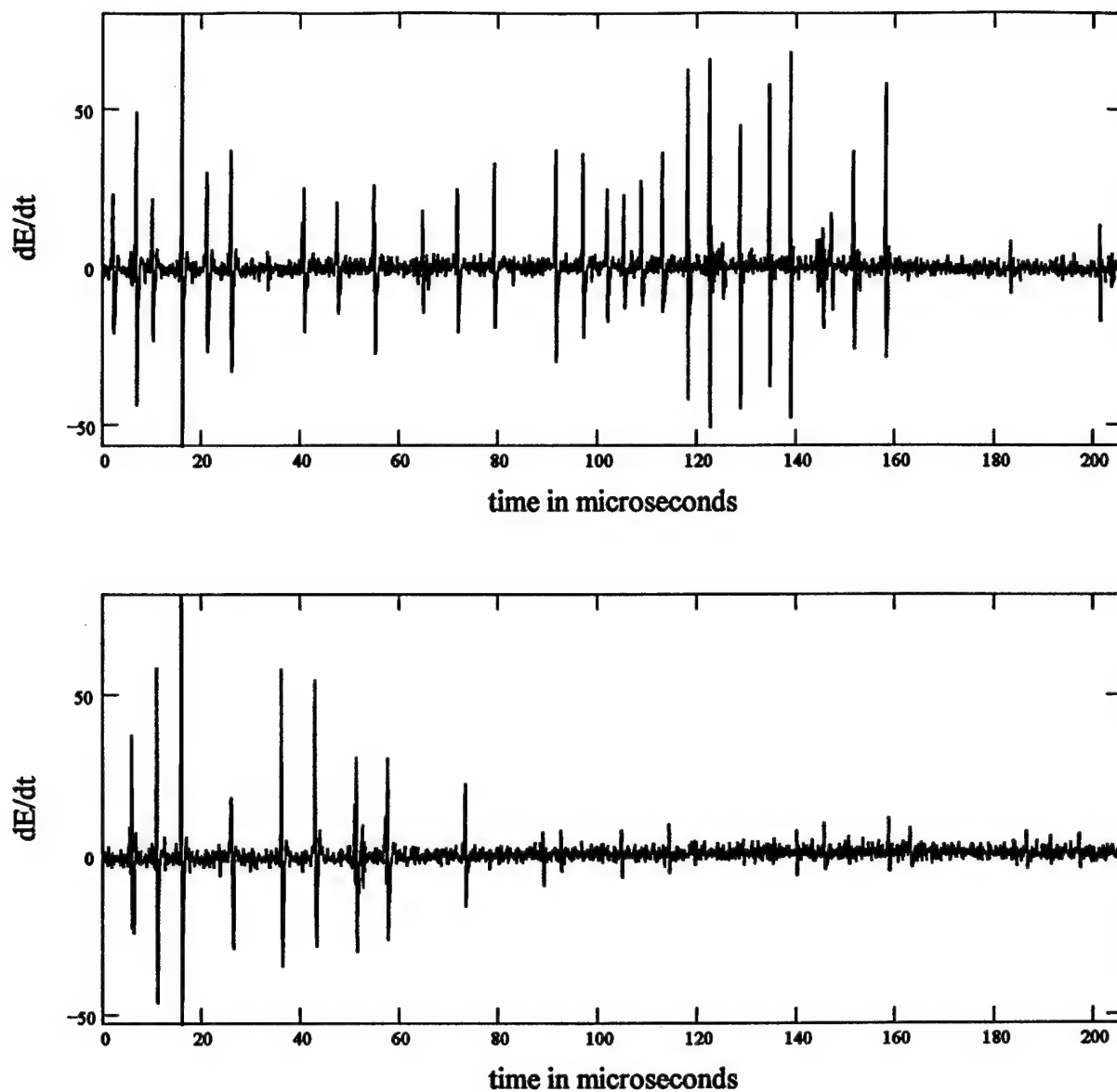


Figure 9. dE/dt waveforms for the final 430 microseconds of the pulse train in flash 2420770 (Time between events is 30 microseconds). Earlier event shown at top.

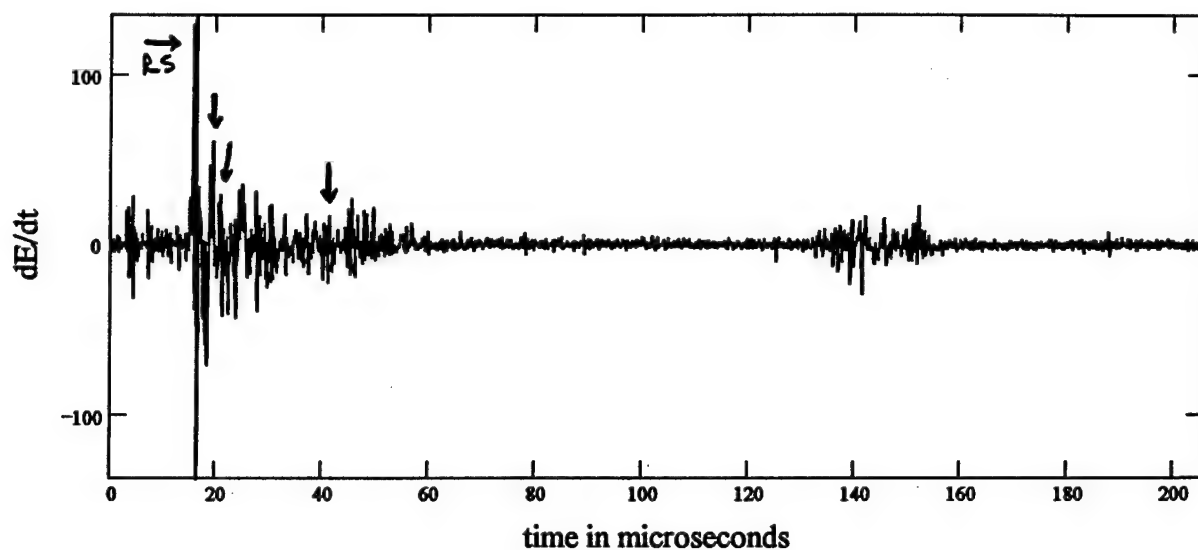


Figure 10. dE/dt waveform for the third stroke in flash 2420770. This stroke occurred 145 ms after the first strokes in the discharge and formed a new termination to ground. The main return stroke peak is marked "RS" as well as locations obtained during the fine structure.

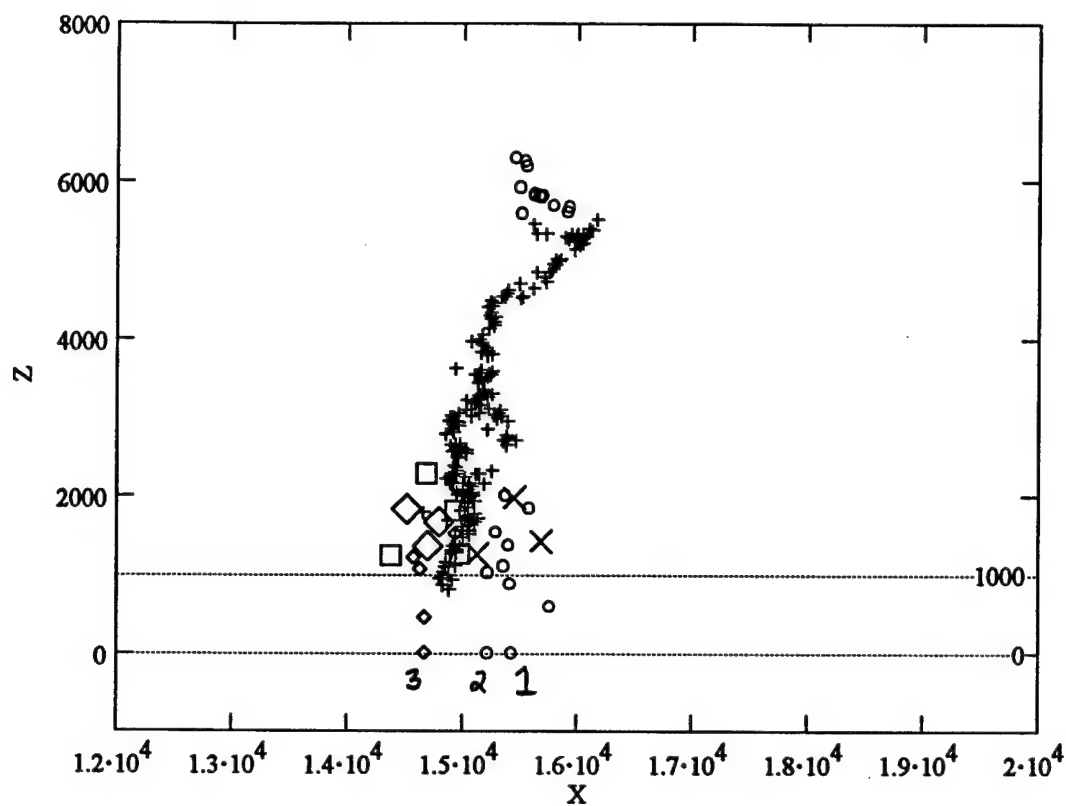
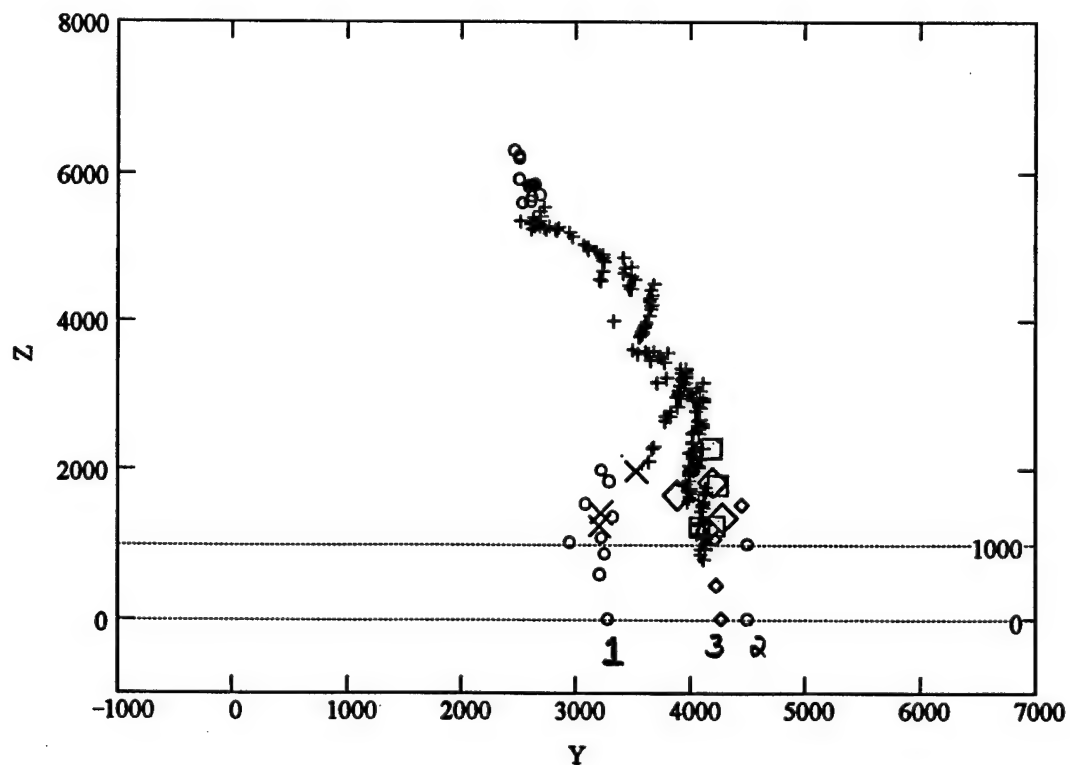


Figure 11 Locations of all dE/dt sources in flash 24200770. Locations of fine structure of new termination are shown as large diamonds. All other symbols are same as mentioned in earlier figures.



of the first stroke were unable to be obtained owing the time offsets among multiple traces. We don't know what happened to the first stroke after the last location we plot, whether it continued higher into the cloud, out along the branch of the second stroke, or both. With regard to the second stroke, we were able to locate the end of the fine structure and it is about 2.3 km high. After this point the second stroke apparently no longer served to discharge branches from the preceding leader. Finally, strokes 4,5 and 6 of the discharge were co-located with the new termination and followed it by 31 ms, 44 ms, and 78 ms respectively.

Ground conductivity effects

The finite conductivity of the ground affects our waveshapes, effectively moving the dE/dt pulses in time. This introduces errors in our source locations. In an effort to understand this phenomenon and correct for these time shifts, we are using existing models in conjunction with our dE/dt waveshapes to find the ground conductivity and correct for its effects. A full description of this project is given in the Final report for F49620-94-1-0256 "Ground conductivity estimated from wideband dE/dt waveshapes of distant lightning sources near ground".

Executive Summary

Personal Supported

Ewen Thomson, Associate Professor
Jamie Stone, Scientific Programmer
Steve Davis, Doctoral student
Jim Schueler, Masters student
David Crawford, Masters student

Publications

Papers presented at American Geophysical Union Fall Meeting, San Francisco, 1995:-

Thomson, E.M. and S. Davis, "Waveshapes in multiple station dE/dt from lightning"

Davis, S. and E.M.Thomson, "Reversal effects in multiple station dE/dt from lightning"

Schueler, J.R., and E.M.Thomson, "Conductivity effects in dE/dt waveshapes from lightning"

Medelius, P. J., Y. Yariv, E.M. Thomson, and S. Davis, "Frequency and phase compensation in a pulse transmission system", NASA Tech. Briefs, March, 1997

Thomson, E.M., "Location of sources of radiation using a weighted hyperbola technique", NASA Tech. Briefs, December, 1997

Thomson, E.M. "Exact expressions for electric and magnetic field from a propagating lightning channel" to be submitted to J. Geophys. Res.

References

- Hager, W.W., and D. Wang, An analysis of errors in the location, current, and velocity of lightning, *J. Geophys. Res.*, **100**, 25,721-25,729, 1995.
- Holmes, C.R., Szymanski, E.W., Szymanski, S.J., and Moore, C.B., Radar and acoustic study of lightning, *J. Geophys. Res.*, **85**, 7517-7532, 1980.
- Guo, C., and E. Krider, The Optical and Radiation Field Signatures Produced by Lightning Return Strokes, *J. Geophys. Res.*, **87**, 8913-8922, 1982.
- Krehbiel, P.R., Brook, M., and McCrory, R., An analysis of the charge structure of lightning discharges to the ground, *J. Geophys. Res.*, **84**, 2432-2456, 1979.
- Koshak, W.J. and E.P. Krider, Analysis of lightning field changes during active Florida thunderstorms, *J. Geophys. Res.*, **94**, 1165-1186, 1989.
- Krider, E.P., and Radda, G.J., Radiation field waveforms produced by lightning stepped leaders, *J. Geophys. Res.*, **80**, 2653-2657, 1975.
- LeVine, D.M., and Meneghini, R., Simulation of radiation from lightning return strokes: The effects of tortuosity, *Radio Science*, **13**, 801-809, 1978.
- LeVine, D.M., and Meneghini, R.A. solution for the electromagnetic field close to a lightning discharge, *International Aerospace and Ground Conference*, Fort Worth, , 1983.
- LeVine, D.M., J.C. Willett, Comment on the transmission-line model for computing radiation from lightning, *J. Geophys. Res.*, **97**, 2601-2610, 1992.
- Lin, Y.T., Uman, M.A., and Standler, R.B., Lightning return stroke models, *J. Geophys. Res.*, **85**, 1571-1583, 1980.
- Mazur, V., and Rust, W.D., Lightning propagation and flash density in squall lines as determined with radar, *J. Geophys. Res.*, **88**, 1495-1502, 1983.
- Nucci, C.A., G. Diendorfer, M.A. Uman, F. Rachidi, M. Ianoz, and C. Mazzetti, Lightning return stroke current models with specified channel-base current: A review and comparison, *J. Geophys. Res.*, **95**, 20,395-20,408, 1990.
- Orville, R.E., and Idone, V.P., Lightning leader characteristics in the thunderstorm research international program (TRIP), *J. Geophys. Res.*, **87**, 11,177-11,192, 1982.
- Proctor, D.E., VHF radio pictures of cloud flashes, *J. Geophys. Res.*, **86**, 4041-4071, 1981.
- Rakov, V.A., and M.A. Uman., Waveforms of first and subsequent leaders in negative lightning flashes, *J. Geophys. Res.*, **95**, 16,561-16,577, 1990c.
- Rubinstein, M., and M.A. Uman, Methods for calculating the electromagnetic fields from a known source distribution: Application to lightning, *IEEE Trans. EMC*, **31**, No. 2, , 1989.
- Rubinstein, M., and M.A. Uman, On the radiation field turn-on term associated with traveling current discontinuities in lightning, *J. Geophys. Res.*, **95**, 3711-3713, 1990.
- Schonland, B.F.J., The lightning discharge, *Handbuch der Physik*, **22**, 576-628, Springer-Verlag, Berlin, 1956.
- Taylor, W.L., A VHF technique for space-time mapping of lightning discharge processes, *J. Geophys. Res.*, **83**, 3575-3583, 1978.
- Thomson, E.M., Galib, M.A., Uman, M.A., Beasley, W.H., Master, M.J., Some features of stroke occurrence in Florida lightning flashes, *J. Geophys. Res.*, **89**, No. D3, 4910-4916, 1984.
- Thomson, E.M., P.J. Medelius, and S.Davis, System for locating the sources of wideband dE/dt from lightning, *J. Geophys. Res.*, **99**, No D11, 22,793-22,802, 1994.
- Thottappillil, R., V.A. Rakov, and M.A. Uman., Distribution of charge along the lightning channel: relation to remote electric and magnetic fields and to return stroke models, *J. Geophys. Res.*, **102**, 6987-7006, 1997.
- Uman, M.A., Lightning return stroke electric and magnetic fields, *J. Geophys. Res.*, **90**, 6121-6130, 1985.
- Uman, M.A., and McLain, D.K., Radiation field and current of the lightning stepped leader, *J. Geophys. Res.*, **75**, 1058-1066, 1970.
- Wangness, R.K., "Electromagnetic Fields", Wiley, New York, 1986.

Weidman, C. D., and E. Krider, The Fine Structure of Lightning Return Stroke Wave Forms, *J. Geophys. Res.*, **83**, 6239-6247, 1978.

Weidman, C.D., and Krider, E.P., The radiation field wave forms produced by intracloud lightning discharge processes, *J. Geophys. Res.*, **84**, 3159-3164, 1979.

Willett, J.C., V.P. Idone, R.E. Orville, C. Leteinturier, A. Eybert-Berard, L. Barret, and E.P. Krider, An experimental test of the "transmission-line model" of electromagnetic radiation from triggered lightning return strokes, *J. Geophys. Res.*, **93**, No.D4, 3867-3878, , 1988.

Willett, J. C., D. Le Vine, and V. Idone, Lightning-channel morphology revealed by return-stroke radiation field waveforms, *J. Geophys. Res.*, **100**, 2727-2738, 1995.

Appendix A

Features of pulse train occurrence

Flash #	Stroke #	Δt (RS) ms	H km	h km	T ms	v(10e6) m/s	T→RS ms	Fine Str μ s	ΔD (RS) km
New-Term									
24402517 (18)	2	170	7	1.0	3.2	1.6-3.0	2.8	46 (110)	0.32
25400631 (19)	2	165	4.6	1.0	1.5	2.4	5.0	74 (124)	0.12
25400638 (25)	2	115	4.7	1.1	2	1.9	1.9	84 (100+)	1.58
25401613 (25)	3	72	4.1	1.0	1.1	3.04	2.7	35 (200)	0.21
25400770 (24)	3'	154	5.3	0.9	2.7	1.8	4.5	40 (150+)	0.63-1.28
25400472 (18)	3'	94	6.2	1.8	1.9		1.4	43 (143)	0.2-1.13
25401713 (25)	2	184	5.1	1.4	1.8	3.6	3.0	70 (150+)	0.5
24402596 (13)	2	116	5.6	0.8	3	1.73	12.0	34 (133)	0.89
24200739 (13)	2	191	2.9	1.9	0.8	1.28	11.0	37 (149)	0.5
24200744 (20)	3'	203	6.5	3.6	1.5	2.15	8.0	44 (159+)	0.36-0.61
25400703 (18)	2	147	4.1	3.0	1	2.2	39.0	164 (167)	2.7
24402546 (23)	2	68	3.5	2.0	*		6.0	48 (100+)	1.36
24200760 (18)	2	71	3.5	0.7	1	2.8	1.0	40 (150+)	0.1-0.9
25401810 (25)	2	91*	3.4	2.3	0.7	1.6	9.0	120 (200)	2.6
Dart-step									
25400642 (25)		93	3.3	0.0	1.3	3.4	0.0	—	—
25400131 (18)			2.1	0.0	1.2	1.8	0.0	—	—
25400651 (25)	2+	143	3.1	0.0	1.2	2.6	0.0	—	—
25400695 (11)	1+	74	3.6	0.0	0.6		0.0	—	—
25401626 (25)	2+	41	3	0.0	1	3	0.0	—	—
25401487 (25)	2	45	4.1	0.0	0.8	5.2	0.0	—	—
	3	33	6	4.0	0.8	2.5	0.2	—	—
25401672 (25)	2	64	4.7	0.0	1.1		0.0	—	—

Legend

- Stroke # - pulse train precedes this stroke in flash; prime indicates first two strokes within
- Δt (RS) - time from previous stroke to start of pulse train
- H (m) - highest sources in pulse train
- h (m) - lowest sources in pulse train
- T (ms) - duration of pulse train
- v (10e6) m/s - average velocity over length of pulse train
- T → RS - time from last source in pulse train to following return stroke
- fine str (μ s) - duration of fine structure; new termination (first stroke in flash)
- ΔD (RS) km - distance between first stroke in flash and new termination

Pulse trains occurring as dart-stepped leaders followed an existing channel completely to gro